

Open orbits on the Fermi surface of tin using the induced-torque method*

A. E. Dixon

Department of Physics, University of Waterloo, Waterloo, Ontario, Canada

(Received 11 November 1974)

Both periodic and aperiodic open orbits have been studied at low fields, with most measurements at 10 kG. Aperiodic open orbits from both the fourth-zone hole surface and the fifth-zone electron surface have been clearly observed and the extent of the two-dimensional regions of magnetic field direction for these orbits has been plotted. The magnetic field dependence and temperature dependence of broad aperiodic open-orbit torque peaks have been used to predict the magnetic field and temperature dependence of two sharp periodic-open-orbit torque peaks and thus to demonstrate that those sharp peaks are caused by periodic open orbits which exist on both the fourth- and fifth-zone surfaces simultaneously. A large number of periodic open orbits which exist along directions of lower symmetry for smaller ranges of magnetic field direction have been observed, many for the first time. The data are compared with the results of other experiments and with theoretical predictions.

I. INTRODUCTION

The Fermi surface of white tin has been investigated for several years, and its topology is known in some detail. The de Haas-van Alphen (dHvA) effect has been studied in detail by several workers (Gold and Priestley,¹ Stafleu and de Vroomen,² and Craven and Stark³) and has yielded a wealth of information. Open orbits on the Fermi surface have been studied using magnetoresistance techniques (Alekseevskii *et al.*,⁴ Anderson and Young,⁵ and Young⁶). Fermi-surface calipers have been accurately measured using the radio-frequency size effect (Gantmakher^{7,8} and Matthey *et al.*⁹).

The induced-torque technique allows the experimenter to plot a complete stereogram of open-orbit directions using only one spherical single crystal, and without the necessity of attaching leads to the sample. The method measures the torque from eddy currents induced in a sample suspended in a slowly rotating magnetic field and was first used by Moss and Datars¹⁰ to investigate open orbits in mercury. A theoretical description of the effect was given by Visscher and Falicov¹¹ and by Lass and Pippard.¹²

At high fields the torque increases proportional to B^2 in the presence of open orbits and saturates when the orbits are closed, as long as there is no magnetic breakdown. In this experiment the torque from closed orbits was so small that it was difficult to detect at all. The open-orbit torque about the y axis due to a magnetic field rotating in the x - z plane, and at the instant when the field is perpendicular to the open-orbit direction in \vec{k} space, is given by¹¹

$$N_y = d_1 B^2 \cos^2 \alpha + d_2, \quad (1)$$

where α is the angle between the open-orbit direction in \vec{k} space and the field rotation plane, and d_1 and d_2 are constants.

This paper reports the results of an induced-torque experiment giving additional information about open orbits on the Fermi surface of tin. The experimental method is described in Sec. II. The Fermi surface of tin is described in Sec. III, and experimental results are presented in Sec. IV. The results of this experiment are compared with the theory and with the results of other experiments in Sec. V.

II. EXPERIMENTAL METHOD

Torques were measured with a self-nulling electronic torque balance like that used by Condon and Marcus¹³ and by Vanderkooy and Datars¹⁴ to detect dHvA-effect torques. The suspension system was modified to allow changes of sample orientation between rotations of the magnet (Moss and Datars¹⁰). The induced torque was generated by rotating a 12-in. Magnion electromagnet at a constant rate using a motor and chain drive (usually at 10°/min), and at constant field strength. Torque signals were recorded directly on an X-Y recorder and were simultaneously stored in digital form on magnetic tape. A computer then compared the data from both directions of magnet rotation, corrected for compliance in the torque magnetometer, and subtracted the data points for one direction of magnet rotation from the corresponding points for the other direction. This had the effect of increasing the induced-torque signal, which is an odd function of magnetic field rotation direction, and reducing signals, which are an even function of rotation direction (e.g., dHvA-effect torque signals and slowly varying background signals from the sample holder). The enhanced result was then plotted on a Calcomp plotter. A complete description of the computer-enhancement technique is given by Grodski and Dixon.¹⁵ The sample was a $\frac{3}{16}$ -in.-diam sphere cut by spark machining from a single crystal of high-purity tin

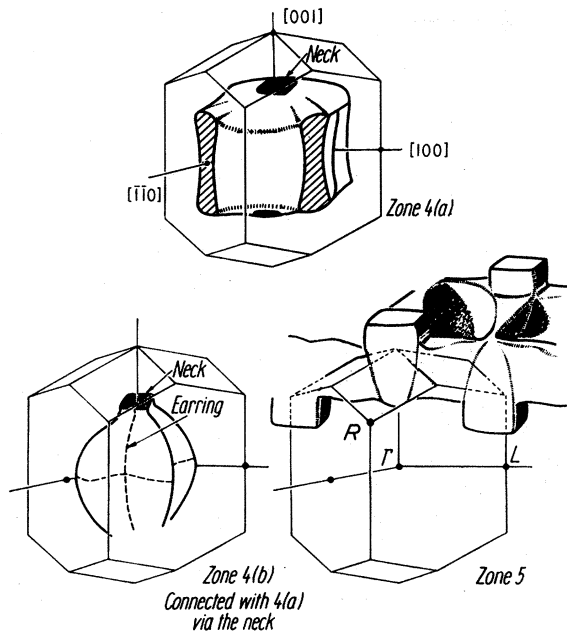


FIG. 1. Fermi-surface model for zones 4 and 5 calculated by Stafleu and de Vroomen. The parts of the Brillouin-zone edges inside the fifth-zone surface are shown dotted; another pear-shaped piece at R (not shown) is connected with an arm to the pear at the top of the zone.

obtained from Materials Research Corp. It was mounted in a micarta barrel and oriented with back-reflection Laué photographs. The sample could be rotated about a horizontal $[100]$ axis oriented so that the magnetic field was along $[100]$ at the beginning of each magnet rotation.

III. FERMI SURFACE OF TIN

White tin has a body-centered-tetragonal lattice with two atoms per unit cell. The low-temperature lattice constants (Weisz¹⁶) are $a = 5.80 \text{ \AA}$ and $c = 3.15 \text{ \AA}$. Most of the sheets making up the Fermi surface of tin are recognizable distortions of the empty-lattice model first described by Gold and Priestley.¹ A local-pseudopotential approximation used by Weisz¹⁶ and based on Gantmakher's^{7,8} size-effect measurements produced a Fermi-surface model qualitatively similar to the later calculations by Stafleu and de Vroomen¹⁷ (based on dHvA-effect measurements²). For the purposes of this experiment, the most important parts of the Fermi surface are the open surfaces in zones 4 and 5, shown in Fig. 1. Zone 4 is made up of two surfaces connected together: a multiply connected hole surface with large arms along $\langle 110 \rangle$, connected to an electron surface centered at Γ by necks at the top and bottom of the two surfaces. The fifth-zone electron surface is a large multiply connected sheet consisting of pear-shaped pieces and connecting arms. Both surfaces are essentially two-dimensional networks

of tubes lying in the (001) plane.

The surface shown in Fig. 1 will support two types of open orbits, periodic and aperiodic. A periodic open orbit occurs when the magnetic field is perpendicular to a symmetry direction along which the Fermi surface is multiply connected. Aperiodic open orbits can occur for a solid angle of magnetic field directions around a symmetry direction in the crystal. In this case the electron's motion is not periodic, and the open orbit is not along a symmetry direction. This solid angle of field directions will be represented by an area on a stereographic projection of field direction along which open orbits are observed, and because of this these orbits are sometimes called two-dimensional aperiodic open orbits (Fawcett¹⁸). In both cases the representative point of the electron must be able to move along the Fermi surface to infinity in the extended zone scheme, while staying in a plane perpendicular to the magnetic field direction.

The two types of open orbits are easily distinguished in a data trace. Periodic open orbits give rise to sharp torque spikes when the magnetic field passes through a direction perpendicular to the open-orbit direction, while aperiodic open orbits result in broad, flat-topped torque peaks as the magnetic field passes through the solid angle of field directions inside which these orbits are observed. Because of the two-dimensional nature of the surface shown in Fig. 1, all periodic open-orbit directions lie in the (001) plane, and both surfaces support aperiodic open orbits for a range of field directions near $[001]$.

The large $\langle 110 \rangle$ -directed arms of the fourth-zone hole surface should give torque spikes for magnetic field directions perpendicular to the (110) directions, except for $[001]$ where all orbits on the surface are closed (a singular field direction, Fawcett¹⁸), and for field directions very near $\langle 110 \rangle$ where the open orbit is closed by the presence of necks joining the fourth-zone electron and hole surfaces. Around $[001]$ aperiodic open orbits will exist for all magnetic field directions for which there exist closed orbits centered at L ; if there are closed orbits centered at L , it is impossible for an electron moving along the top of the sheet to get to the bottom and reverse its direction to form a closed orbit. Instead, it will continue to move with the same average direction on the top half of the sheet. The disappearance of the closed orbit can thus be used to predict the size and shape of the area of aperiodic open orbits on the stereogram. The region of aperiodic open orbits will result in a large, broad torque peak whenever \vec{B} sweeps through the region of aperiodic open orbits around $[001]$. The fourth-zone surface will also support a narrow band of periodic open orbits along $\langle 100 \rangle$, because of the thickness of the connecting arms.

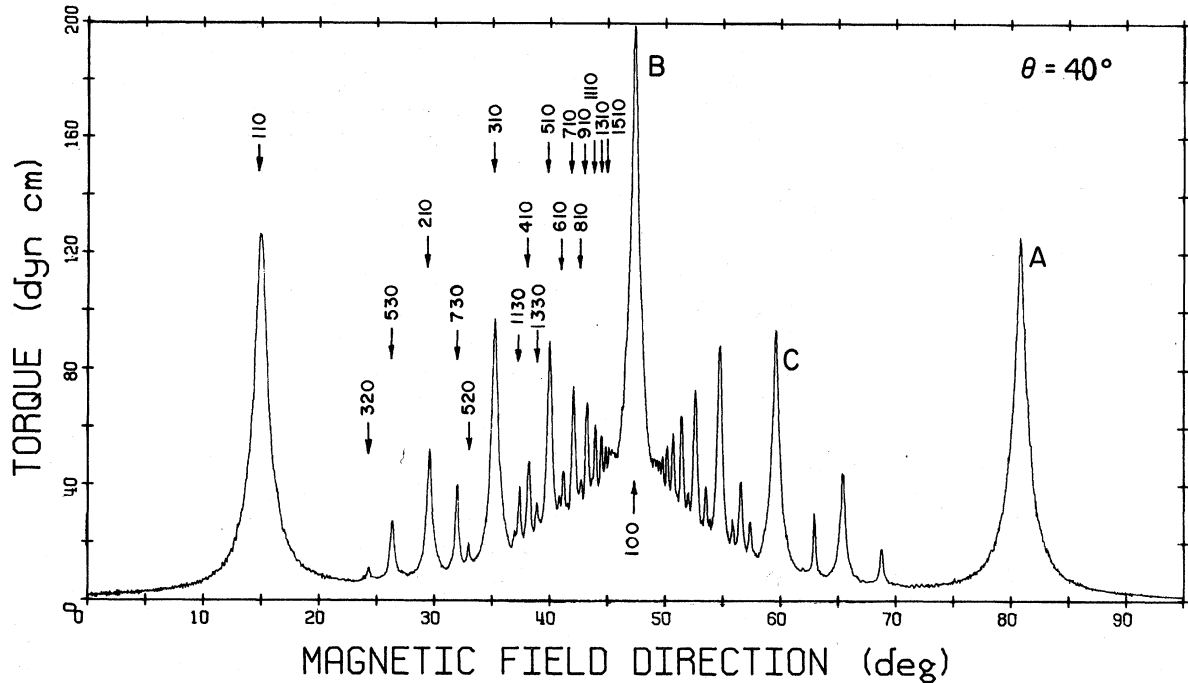


FIG. 2. Data trace as the magnetic field sweeps through the edge of the aperiodic-open-orbit region. The magnetic field rotation plane is tilted 40° from $[001]$ about $[010]$. Torque peaks are labeled to show the direction of the open orbit causing the peak, not the direction of the magnetic field in this rotation plane.

The fifth-zone electron surface should give torque spikes whenever \vec{B} is perpendicular to $[100]$, except for the singular field direction along $[001]$, and broad torque peaks for a two-dimensional region around $[001]$. Because the arms are thinner than those of the fourth-zone surface, the two-dimensional region will be smaller than for the fourth-zone surface. This region of aperiodic open orbits will result in a second broad torque peak superimposed on the broad peak from the fourth zone, but it will be somewhat narrower because the two-dimensional region is smaller. The model also predicts a narrow band of periodic open orbits for \vec{B} along $[110]$.

A further calculation by Craven¹⁹ was based on dHvA-effect measurements by Craven and Stark,³ and in a discussion of the magnetoresistance results by Alekseevskii *et al.*⁴ and Anderson and Young⁵ makes several theoretical predictions that can be compared with the present experiment. The most recent calculation by Devillers *et al.*²⁰ is based on the extensive radio-frequency-size-effect data by Matthey *et al.*⁹ Both of these models are qualitatively similar to that shown in Fig. 1.

IV. EXPERIMENTAL RESULTS

A survey of open-orbit directions was performed at 10 kG and 1.2 °K by rotating the sample through 2° intervals about $[010]$ after each pair of magnet rotations until a complete stereogram of field di-

rections was obtained. A portion of one such rotation plot is shown in Fig. 2, where the magnetic field is rotating in a plane tilted 40° from $[001]$ toward $[100]$. Each open-orbit torque spike on the diagram is plotted as a point on the stereogram of open-orbit directions shown in Fig. 3. The curve labeled $\theta = 40^\circ$ corresponds to the data trace shown in Fig. 2. The large spikes on the right and left of Fig. 2 (labeled A) are from the $\langle 110 \rangle$ -directed orbits, and the spike at the center of the diagram (labeled B) is from one of the $\langle 100 \rangle$ -directed orbits. Note that these labels do not correspond to magnetic field directions in this diagram, but instead to open-orbit directions whose torque spikes are visible for a range of field directions in the plane perpendicular to the open-orbit direction. These (A and B) are the major open orbits in tin and can be seen for almost all rotation planes except for field directions very near the $[001]$ singular field direction. When the magnetic field is rotated in the (001) plane ($\theta = 90^\circ$), only A and B are seen. C is first visible as a very small blip in the curve for $\theta = 60^\circ$, and the series of smaller spikes between A and B appear as the magnet rotation plane is changed so that the magnetic field sweeps closer and closer to $[001]$. They are visible for short ranges of field direction, and the data points for each spike fall on radial lines on the stereogram. The lines represent planes whose poles lie on the outer circle of the stereogram, and correspond to open-orbit

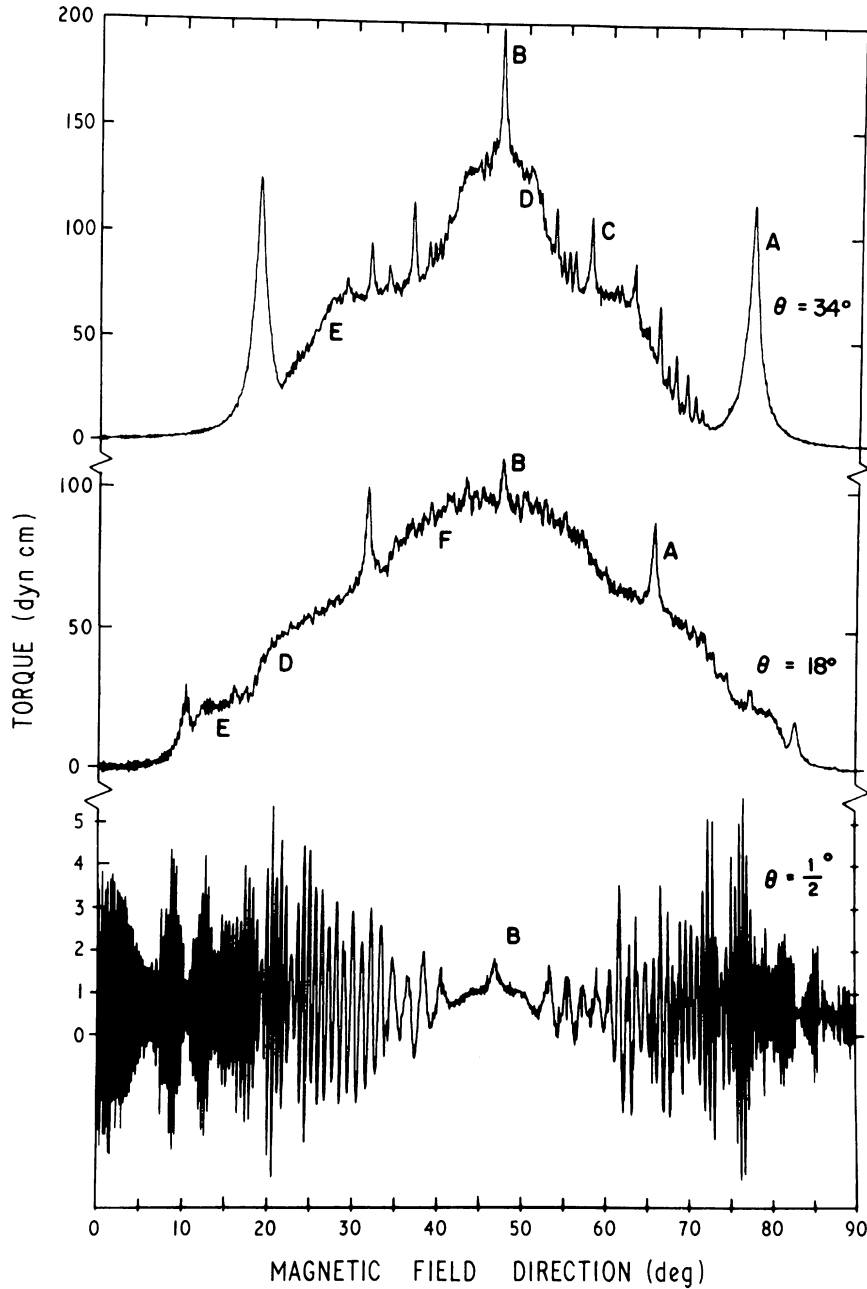


FIG. 4. Top trace shows aperiodic-open-orbit peak D superimposed on aperiodic-open-orbit peak E. The middle trace shows part of a magnet rotation in which B passes well inside the aperiodic-open-orbit regions, and in the bottom trace the magnetic field passes $\frac{1}{2}^\circ$ from [001], showing the decrease in torque signal near the singular field direction.

the curve closest to [001] shows the edges of peak F. The extent of the aperiodic open-orbit region on the fourth-zone hole surface was computed using the empty-lattice model for the Fermi surface. (A computer program by Taylor²² was adapted to provide plots on the Calcomp plotter at the University of Waterloo.) The results are plotted as plus signs. A similar calculation for the fifth-zone surface obtained the limits of the aperiodic-open-orbit region in the $\langle 100 \rangle$ directions: this data is shown as crosses, but is not expected to be very reliable, because the empty-lattice-model prediction of the

fifth-zone surface is poor.

The amplitudes of the torque peaks from the [010]-, $[1\bar{1}0]$ -, and $[3\bar{1}0]$ - directed open orbits are plotted as a function of magnetic field direction (measured in degrees from [001]) in Figs. 6, 7, and 8. In Fig. 6 the magnetic field direction is the same as the angle θ in the data traces of Figs. 2 and 4, however, this is not the case in Figs. 7 and 8 (except at 0° and 90°). In Figs. 6, 7, and 8 a field direction of 0° corresponds to a rotation plane where \vec{B} passes through the singular field direction [001] where the torque peaks have disappeared. A

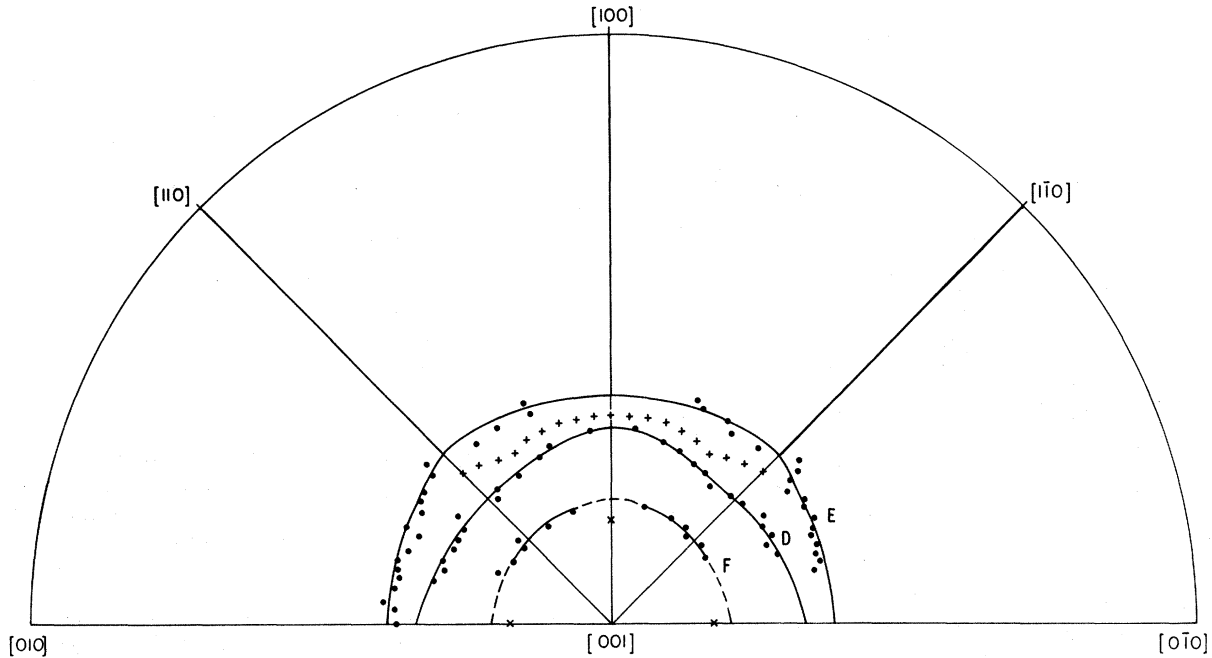


FIG. 5. Stereogram of measured limits of the electron surface aperiodic-open-orbit region (D) and the hole-surface aperiodic-open-orbit region (E). F shows limits of a third broad peak superimposed on E and D. Limits of the fourth-zone (+) and fifth-zone (x) aperiodic-open-orbit regions were calculated using the empty-lattice model.

field direction of 90° in these figures corresponds to the situation where $\theta = 90^\circ$ and the magnetic field rotates in the (001) plane.

To see how these three curves are plotted, consider the data shown in the top trace of Fig. 4. The [100]-directed orbit (spike B) is superimposed on peak D, which in turn is sitting on peak E. The magnetic field direction at spike B is tilted 34° from [001] toward [100], so these three points are plotted at 34° in Fig. 6. Spike A occurs 29° from spike B on a trace tilted 34° from [001] about [010], so the position of this spike corresponds to a magnetic field direction tilted 43.7° from [001] toward [110], and is plotted at 43.7° in Fig. 7. Spike C occurs 10.6° from B on the $\theta = 34^\circ$ trace, it is plotted at 35.4° in Fig. 8.

Since the fifth-zone electron surface is multiply connected with arms along $\langle 100 \rangle$, it will support open orbits for a large range of field directions which are perpendicular to $\langle 100 \rangle$. This would result in a torque spike at the positions where the peak B has been observed in this experiment. In addition, it may be possible for the fourth-zone hole surface to support open orbits along $\langle 100 \rangle$, even though it is multiply connected by arms along $\langle 110 \rangle$, if the arms are thick enough. In that situation, spike B would be caused by open orbits on both the fourth-zone hole surface and the fifth-zone electron surface acting simultaneously for some magnetic field directions. Using a similar argu-

ment, spike A may be caused by open orbits on the fifth-zone electron surface, if its arms are thick enough, as well as the orbit expected on the fourth-zone hole surface for most field directions perpendicular to $\langle 110 \rangle$. In order to investigate the possibility of open orbits occurring on two different surfaces simultaneously, first consider the top data trace shown in Fig. 4. Peak D results from aperiodic open orbits on the thin arms of the fifth-zone electron surface, while the broader peak E

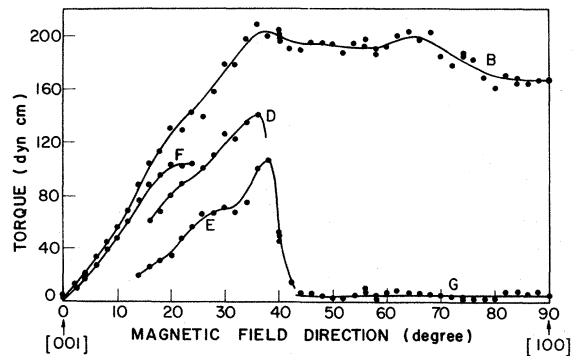


FIG. 6. Amplitude of the torque spike from the [010]-directed open orbit (B) as a function of magnetic field direction. D, E, and F show the amplitude of the broad torque peaks lying below B in the data trace. The residual background signal from closed orbits is shown as curve G.

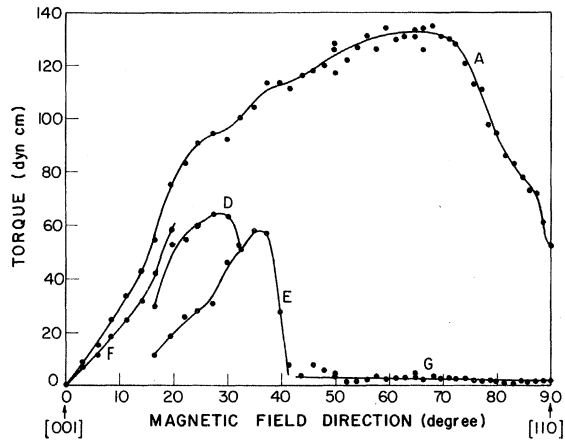


FIG. 7. Amplitude of the torque spike from the $[1\bar{1}0]$ -directed open orbit (A) as a function of magnetic field direction. D, E, F, and G are background torques lying below spike A.

results from aperiodic open orbits on the thicker arms of the fourth-zone hole surface. Since peak D can be attributed to the fifth-zone electrons acting alone, and peak E to the fourth-zone holes acting alone, if these peaks behave differently as some experimental variable is changed, it should be possible to use this behavior to prove whether A and B are caused by both electron and hole orbits simultaneously, or are due to only one type of carrier. Both the magnetic field strength and the temperature can be varied in this experiment, and since D and E show different behavior as the field strength and temperature are varied, the results of both of these experiments are described.

In order to plot the torque amplitude as a function of magnetic field strength, a decision on how to plot the correct amplitude of spike B must be made. Broad peak D can be attributed to the fifth-

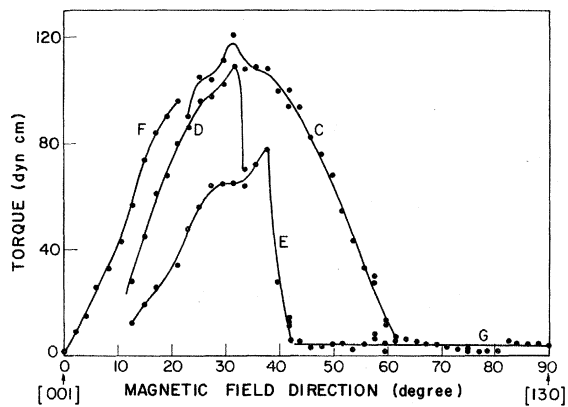


FIG. 8. Amplitude of the torque spike from the $[3\bar{1}0]$ -directed open orbit (C) as a function of magnetic field direction. D, E, F, and G are background torques.

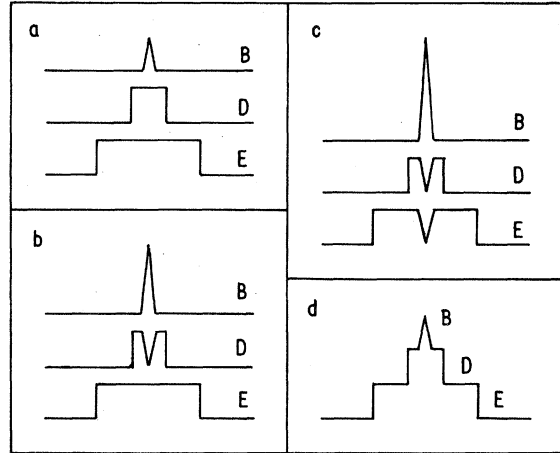


FIG. 9. (a), (b), and (c) show three different ways to add the superimposed torque signals B, D, and E to produce the observed signal (d).

zone electrons and the broader peak E to the fourth-zone holes, and the conductivity caused by orbits on these two surfaces is additive and so the induced torque is additive as well. In this case the height of broad peak D is measured above the top of broad peak E, while peak E is measured above the closed-orbit base line (essentially zero torque in this experiment). Three possibilities, each of which gives a different plotting height for spike B, are shown schematically in Figs. 9(a), 9(b), and 9(c). In each case the three curves add up to the observed result [Fig. 9(d)]. Figure 9 shows the situation in which B is treated in exactly the same way as D and E, and this the obvious first approach. Figure 9(b) shows what would happen if spike B were caused only by a periodic open orbit on the fifth-zone electron surface (which is multiply connected along the $\langle 100 \rangle$ directions). As the magnetic field sweeps from left to right across the diagram, it first reaches the edge of the aperiodic-open-orbit region on the fourth-zone hole surface, and the induced torque increases at the edge of broad peak E. Next it reaches the edge of the region of aperiodic open orbits on the fifth-zone electron surface, and begins to trace out peak D. If the periodic open orbit is on the fifth-zone surface but not on the fourth, the electrons contributing to the current along the aperiodic open orbits will be the same carriers that carry current along the periodic-open-orbit direction, and just at that direction the current is all carried along the periodic open orbit and the torque from the aperiodic orbits drops to zero. Meanwhile, the torque from aperiodic open orbits on the fourth-zone hole surface would still exist. Another possibility that gives the same result for the height of spike B, is a flat top for D and a drop to zero torque at the center of peak E. Since the fifth-zone

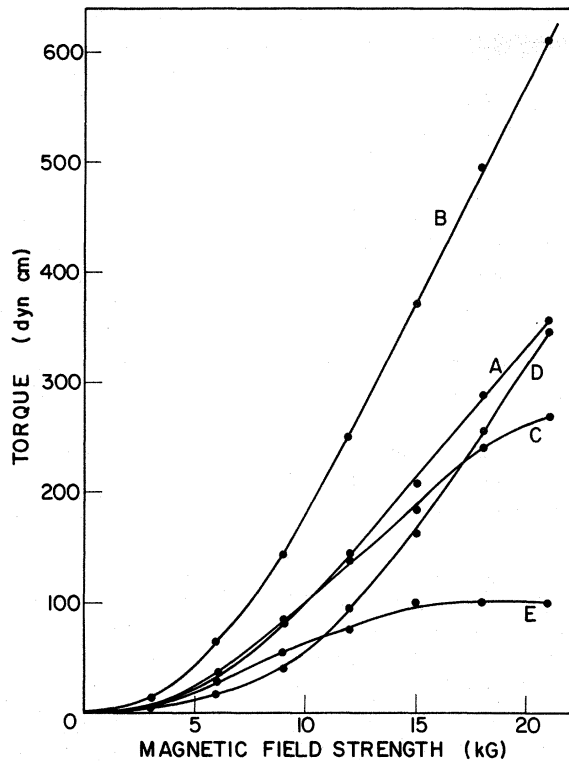


FIG. 10. Peak height versus magnetic field strength for data at $\theta = 33^\circ$ using the model of Fig. 9(c).

surface is multiply connected with arms along $\langle 100 \rangle$, it would almost certainly support open orbits along $\langle 100 \rangle$; this possibility was not considered. Figure 9(c) shows what will happen if the aperiodic open orbits on both surfaces become periodic along $[100]$: The torque from the aperiodic open orbits drops to zero when the same carriers start moving along the periodic open orbits, and in this case the height of peak B should be measured above the base line.

As the magnetic field rotation plane is changed from (001) , where the magnetic field direction passes through $[100]$ at a magnetic field direction of 90° in Fig. 6, peak E appears under B at a magnetic field direction of 42° and D appears a few degrees later. Both of these peaks grow in amplitude very quickly. As the rotation plane of the magnet is changed through this region, the three possible mechanisms proposed to explain spike B in Figs. 9(a), 9(b), and 9(c) should all give different results. In Fig. 9(a) spike B would ride up on top of peak E and then peak D as they appeared underneath it, so that the total induced torque measured at the tip of B would be considerably increased by the appearance of D and E beneath it. In Fig. 9(b), spike B should ride up on E, but its amplitude would be unaffected by the appearance of D. Finally, in Fig. 9(c) the total height of B should be unaffected by the appearance of D and E. Figure 6 shows that the

appearance of E and then D has very little effect on the height of B as the angle between the field direction and $[001]$ is decreased, indicating that the mechanism described in Fig. 9(c) is much more plausible than that in either Fig. 9(a) or 9(b), and that the full height of spike B should be plotted in an amplitude versus magnetic field plot.

The amplitude of the five peaks labeled in Fig. 4 is plotted as a function of magnetic field strength in Fig. 10 (for $\theta = 33^\circ$), with the height of A, B, C, and E measured above the zero level, and peak D is measured above the flat top of E. Of the five peaks plotted, only two behave in the usual way; peak D shows a nearly-quadratic field dependence, which is expected for open orbits^{11,12} (the actual field dependence is approximately $B^{2.2}$), and peak E shows definite saturation from the magnetic breakdown²³ in the fourth-zone hole surface which has previously been observed in magnetoresistance experiments in tin.^{5,6} Spike C appears to be beginning to saturate as the field is increased, but the most startling behavior is the almost-linear increase in amplitude of A and B above 12 kG. If the decision that spike B was caused by both electrons and holes simultaneously is correct, it should be possible to combine the field dependence of the holes (peak E) and the electrons (peak D) to generate the magnetic field dependence of B. If a simple linear combination of D and E is used, the results are shown in Fig. 11. The sum of the amplitude of D and E is fitted to the highest-field data point by adjusting a multiplicative constant, then lower-field values are calculated using that constant and the previously measured field dependence of D and E. The lower pair of curves results when the same procedure is followed for peak A. In both cases the agreement between the field dependence of the calculated and measured curves is excellent. When the temperature dependence of D and E is measured, they act quite differently (see Fig. 12). As the temperature is lowered from 4.2 to 1.2 °K, peak D increases in height by a factor of 2.2, while E increases by a factor of 1.4. As was the case with the field dependence, the temperature dependence of A and B is similar, and can be predicted reasonably well using the temperature dependence of D and E and the constant calculated in Fig. 11.

The Fermi-surface models^{16,17,19,20} predict that the fifth-zone electron surface will support open orbits for all field orientations in the (100) plane, and will support a narrow band of open orbits for magnetic fields in the $[110]$ direction. The fourth-zone hole surface is multiply connected along the $\langle 110 \rangle$ directions, but Craven¹⁹ and Devillers *et al.*²⁰ predict that the neck joining the electron and hole surfaces in zone 4 will cut off the open orbits when the field is along $[110]$, and that the surface will support a narrow band of open orbits when the field

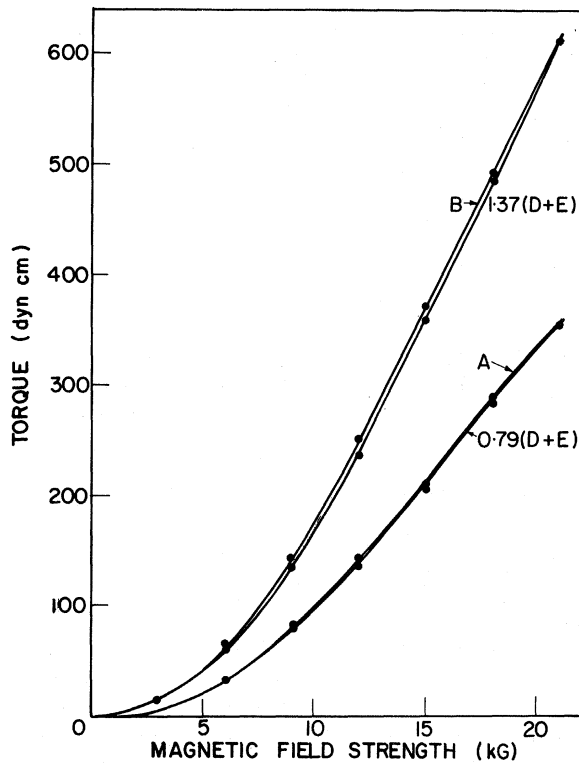


FIG. 11. Simple linear combination of the torque amplitudes of aperiodic-open-orbit peaks D and E is used to predict the magnetic field dependence of periodic-open-orbit spikes A and B.

is along [100]. Thus if the magnetic field is rotated in the (001) plane, the [110] torque spike (B) depends on a broad band of electrons and a narrow band of holes. The field dependence of the two torque spikes was found to be the same, each varying as $B^{1.5}$. The peaks also exhibit similar temperature dependence. In both cases the amplitude increased by a factor of 1.5 as the temperature was reduced from 4.2 to 1.2°K. Because this rotation plane is well outside the region where magnetic breakdown has been observed,⁵ the similar field dependence is not surprising, but the complete disappearance of the holes contributing to the [110] torque spike might be expected to result in a different temperature dependence for that spike, although the difference in temperature dependence of the electrons and holes is not large (see Fig. 12). It is not possible to draw a definite conclusion from this data about whether the holes contributing to the [110] spike have completely disappeared when the field is along [110].

V. COMPARISON WITH OTHER WORK

The extent of the aperiodic regions has been measured directly in transverse magnetoresistance experiments^{4,5} and can be inferred from the cutoff of

the closed orbit enclosing the space between the arms of the open surfaces, which can be measured with the dHvA effect.³ Results from these two experiments, as well as theoretical predictions,¹⁹ are compared with the present measurements in Table I. [The present experiment measures the limit of the fifth-zone region to be 34° and that of the fourth-zone region to be 42° in the (130) plane.] The number in parentheses in the last column is taken from Fig. 5, and is slightly larger than the value from Fig. 7. In the other cases, results from Figs. 6 and 7 agreed with Fig. 5. The edges of the fourth-zone hole surface can be measured more accurately from Figs. 6 and 7 because the data points shown in Fig. 5 come from the rather indistinct outer edges of the broad peak, however the edges of the fifth-zone peak are quite sharp (see Fig. 4) and the data points in Fig. 5 are more precise. These results are in every case but one larger than the results predicted by Craven¹⁹ which in turn were always larger than the dHvA-effect measurements of Craven and Stark.³ The fact that the dHvA-effect measurements are smaller than expected is not surprising, since they are the result of the disappearance of an orbit. At some point the signal from the orbit is too weak to measure, but may not have disappeared completely, so the dHvA signal will disappear slightly before the orbit does. In the present experiment, the edges of the torque peaks were measured by finding the angles at which the torque just starts to increase—for example, in the top trace in Fig. 4, the edges of the peak E were taken to be at 14° and 73° and the edges of peak D 38° and 58°. Other choices for the edge of the peak would result in smaller two-dimensional regions on the stereogram. The magnetoresistance measure-

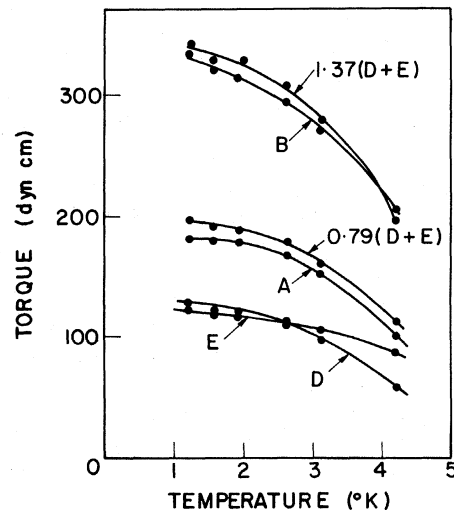


FIG. 12. Same linear combination of the temperature dependence of D and E is used to predict the temperature dependence of A and B.

TABLE I. Limiting angles for the aperiodic-open-orbit regions.

Surface	Plane of \vec{B}	Magneto-resistance ⁵ (deg)	dHvA ³ (deg)	Theory ¹⁹ (deg)	This experiment (deg)
fourth-zone	(100)	38	35	36	43
holes	(110)	44	37	42	42(44)
fifth-zone	(100)	38	35	36	37
electrons	(110)	37	24	25	33

ments⁵ could not differentiate between the two regions in the (100) plane, and measurements were made at higher field strength, a situation which would accentuate the effect of the electron orbits. The data points labeled F in Fig. 5 occur at the same position as anomaly II in the magnetoresistance experiment of Anderson and Young,⁵ but experiment over a wider range of field strengths are necessary to confirm that they result from the same mechanism.

Periodic open orbits exist on the fifth-zone surface for all magnetic field directions perpendicular to [100], except [001], and because of the thickness of the arms, the fourth-zone surface is also open in the same direction for the same range of magnetic field directions.^{19,20} The smooth behavior of spike B near [100] in Fig. 6 supports the contention that the fourth-zone surface supports a narrow band of open orbits for \vec{B} along [100], in addition to a broad band of open orbits on the fifth-zone surface. This is in agreement with the magnetoresistance results⁵ and with Hall-effect measurements by Kachinskii.²⁴ The existence of simultaneous open orbits on both surfaces when $\theta = 33^\circ$ has been clearly demonstrated in this experiment by combining the dependence of torque amplitude on field strength for the aperiodic electron and hole orbits to predict the field dependence of torque peak B (see Fig. 11). A similar technique was used to predict the temperature dependence of B (see Fig. 12).

The fourth-zone hole surface is multiply connected by arms in the $\langle 110 \rangle$ directions, and should support periodic open orbits along [110] for all magnetic field directions perpendicular to [110] except for directions very close to [110], when the open orbit is closed by the neck that joins the fourth-zone electron and hole surfaces.^{19,20} According to Craven's model,¹⁹ a broad band of open orbits along [110] exists on this surface for field orientations up to 71° from [001] in the (110) plane, after which a narrow band of open orbits will exist to within 2.5° of [110]. The sudden drop in amplitude of torque spike A in the vicinity of 71° in Fig. 7 is due to this change from a broad to a narrow band of open orbits on the fourth-zone surface, which has also been seen by Anderson and Young.⁵ The further

drop in amplitude at 88° in Fig. 7 may be due to the complete disappearance of the orbit on the fourth-zone surface, leaving only an open orbit on the fifth-zone surface for \vec{B} along [110]. A study of the temperature and field dependence of this peak at [110] did not prove conclusively that the hole orbit had completely disappeared.

A large number of periodic open orbits have been observed over shorter ranges of field directions, some of which have been followed inside the region where aperiodic open orbits exist on both the fourth and fifth-zone surfaces. The maximum angle from [001] at which each torque peak was observed is compared with the maxima for the four orbits seen by Alekseevskii *et al.*⁴ and predicted theoretically by Craven.¹⁹ (See Table II.) The limiting angle for the [130] orbit on the fourth-zone surface was calculated by Craven to be 61, and that predicted for the fifth-zone surface was 57. The small bump on the amplitude curve in Fig. 8 at 58° may be caused by this change in character of the orbits causing the peak, but a change of slope of the curve would be more reasonable. When the [150] and [120] amplitude curves were plotted in the range

TABLE II. Limiting angles for observing periodic open orbits in particular symmetry planes.

Plane of \vec{B}	Theory ¹⁹ (deg)	Magnetoresistance ⁴ (deg)	This experiment (deg)
(9 7 0)			42
(4 3 0)			42
(7 5 0)			43½
(3 2 0)	47	47	46
(11 7 0)			41
(5 3 0)			46½
(9 5 0)			42½
(2 1 0)	51	52	51
(7 3 0)			44
(5 2 0)			41½
(3 1 0)	61	61	61
(11 3 0)			42
(4 1 0)			44½
(13 3 0)			41½
(5 1 0)	49	53	51
(6 1 0)			42
(7 1 0)			46½
(8 1 0)			41
(9 1 0)			43½
(11 1 0)			42½
(13 1 0)			41½
(15 1 0)			41

near the cut-off angle, there was no evidence of either a slope change or a bump at the predicted limiting angle for orbits on the fifth-zone surface. The reason many of the orbits along directions of lower symmetry were not seen in previous magnetoresistance experiments is probably due to the inherent advantage in high-conductivity materials of a technique that measures conductivity (like the induced-torque effect) over a technique that measures resistance. Many of these peaks are in a region where the background conductivity due to aperiodic open orbits is large, and the increased conductivity due to periodic open orbits can be easily observed in a conductivity measurement but in a resistance measurement shows up as a slight further lowering of an already very small resistance. A further advantage of the induced-torque effect in a soft crystal like tin is the absence of leads which must be attached to the sample to supply current and measure voltage in a magnetoresistance experiment, and the consequent absence of possible damage to the sample during this procedure.

VI. CONCLUSIONS

Open orbits on the Fermi surface of tin have been studied in some detail at 10 kG. Aperiodic-open-orbit regions from both the fourth-zone hole surface and the fifth-zone electron surface have clearly identified, and the extent of these regions has been plotted on a stereographic projection. This experiment shows that the aperiodic-open-orbit region is larger than predicted by theory,¹⁹ especially for the fifth-zone electron surface in the (110) plane, and the size and shape of the aperiodic open-orbit region is different from the magnetoresistance measurements,⁵ which were unable to differentiate between fourth- and fifth-zone aperiodic open orbits in all directions.

This experiment confirms that the fifth-zone surface supports periodic open orbits for all magnetic field directions perpendicular to [110] except for the singular field direction [001]. The fourth-zone surface was found to support periodic open orbits for magnetic field directions perpendicular to [100] (except for [001]) and the dependence of torque amplitude on angle in Fig. 7 supports Craven's¹⁹ prediction that a broad band of open orbits along [110] exists on the fourth-zone surface up to an angle of 71° from [001], after which a narrow band exists to within 2½° of [110]. The temperature and field dependence of the broad aperiodic-open-orbit torque peaks have been combined to predict the temperature and field dependence of spikes *A* and *B* of Fig. 4, and thus, to demonstrate that these are caused by open orbits that occur simultaneously on the fourth- and fifth-zone surfaces. The change in character of the open orbit near 71° was clearly demonstrated by Anderson and Young,⁵ since the approximate compensation of orbits on the two surfaces produced a spike in the magnetoresistance results which changed to a minimum for angles greater than about 72° when the broad band of hole orbits changed to a narrow band.

A large number of open orbits that occur for shorter ranges of magnetic field directions have been observed, many of which have not been observed in previous experiments. The limiting angle from [001] for these orbits has been measured, and for the four orbits observed previously, excellent agreement is found with the magnetoresistance measurements⁴ and theoretical predictions.¹⁹

These measurements are continuing at higher magnetic field strengths and over a wider range of temperatures. A comprehensive study of magnetic breakdown in tin will be made, and an attempt will be made to observe quantum oscillations in the conductivity similar to those seen by Young.⁶

*Research supported by the National Research Council of Canada.

¹A. V. Gold and M. G. Priestly, *Philos. Mag.* **5**, 1089 (1960).

²M. D. Stafleu and A. R. de Vroomen, *Phys. Status Solidi* **23**, 675 (1967).

³J. E. Craven and R. W. Stark, *Phys. Rev.* **168**, 849 (1968).

⁴N. E. Alekseevskii, Yu. P. Gaidukov, I. M. Lifshitz, and V. G. Peschanskii, *Zh. Eksp. Teor. Fiz.* **39**, 1201 (1960) [*Sov. Phys.-JETP* **12**, 837 (1961)].

⁵J. Gerald Anderson and R. C. Young, *Phys. Rev.* **168**, 696 (1968).

⁶R. C. Young, *J. Phys. C* **4**, 474 (1971).

⁷V. F. Gantmakher, *Zh. Eksp. Teor. Fiz.* **44**, 811 (1963). [*Sov. Phys.-JETP* **17**, 549 (1963)].

⁸V. F. Gantmakher, *Zh. Eksp. Teor. Fiz.* **46**, 2028 (1964) [*Sov. Phys.-JETP* **19**, 1366 (1964)].

⁹M. M. M. P. Matthey, M. A. C. Devillers, and A. R.

de Vroomen, *Phys. Status Solidi B* **63**, 279 (1974).

¹⁰J. S. Moss and W. R. Datars, *Phys. Lett. A* **24**, 630 (1967).

¹¹P. B. Visscher and L. M. Falicov, *Phys. Rev.* **213**, 1518 (1970).

¹²J. S. Lass and A. B. Pippard, *J. Phys. E* **3**, 139 (1970).

¹³J. H. Condon and J. H. Marcus, *Phys. Rev.* **134**, 446 (1964).

¹⁴J. Vanderkooy and W. R. Datars, *Phys. Rev.* **156**, 671 (1967).

¹⁵J. J. Grodski and A. E. Dixon (unpublished).

¹⁶Gideon Weisz, *Phys. Rev.* **149**, 504 (1966).

¹⁷M. D. Stafleu and A. R. de Vroomen, *Phys. Status Solidi* **23**, 683 (1967).

¹⁸E. Fawcett, *Adv. Phys.* **13**, 139 (1964).

¹⁹J. E. Craven, *Phys. Rev.* **182**, 693 (1969).

²⁰M. A. C. Devillers, M. M. M. P. Matthey, and A. R. de Vroomen, *Phys. Status Solidi B* **63**, 471 (1974).

²¹S. J. Michalak, M. S. thesis (University of Waterloo, 1974) (unpublished).

²²Roger Taylor, Can. J. Phys. 46, 1403 (1968).

²³W. R. Datars and J. R. Cook, Phys. Rev. 187, 769

(1969).

²⁴V. N. Kachinskii, Zh. Eksp. Teor. Fiz. 43, 1158 (1962). [Sov. Phys.-JETP 16, 818 (1963)].